Climate Feedback Variance and the Interaction of Aerosol Forcing and Feedbacks

A. GETTELMAN

National Center for Atmospheric Research,[a] *Boulder, Colorado*

L. LIN

National Center for Atmospheric Research, Boulder, Colorado, and College of Atmospheric Sciences, Lanzhou University, Lanzhou, China

B. MEDEIROS AND J. OLSON

National Center for Atmospheric Research, Boulder, Colorado

(Manuscript received 18 February 2016, in final form 16 May 2016)

ABSTRACT

Aerosols can influence cloud radiative effects and, thus, may alter interpretation of how Earth's radiative budget responds to climate forcing. Three different ensemble experiments from the same climate model with different greenhouse gas and aerosol scenarios are used to analyze the role of aerosols in climate feedbacks and their spread across initial condition ensembles of transient climate simulations. The standard deviation of global feedback parameters across ensemble members is low, typically 0.02 $\mathrm{W\,m^{-2}\,K^{-1}}$. Feedbacks from high (8.5 $\mathrm{W\,m^{-2}}$) and moderate (4.5 $\mathrm{W\,m^{-2}}$) year 2100 forcing cases are nearly identical. An aerosol kernel is introduced to remove effects of aerosol cloud interactions that alias into cloud feedbacks. Adjusted cloud feedbacks indicate an ''aerosol feedback'' resulting from changes to climate that increase sea-salt emissions, mostly in the Southern Ocean. Ensemble simulations also indicate higher tropical cloud feedbacks with higher aerosol loading. These effects contribute to a difference in cloud feedbacks of nearly 50% between ensembles of the same model. These two effects are also seen in aquaplanet simulations with varying fixed drop number. Thus aerosols can be a significant modifier of cloud feedbacks, and different representations of aerosols and their interactions with clouds may contribute to multimodel spread in climate feedbacks and climate sensitivity in multimodel archives.

1. Introduction

Cloud feedbacks, the cloud response to forced environmental (surface temperature) changes, are the largest uncertainty in estimates of the response of the climate system to radiative forcing (Boucher et al. 2013). Forcing is an imposed change on the system (or the radiative result of an imposed change) and feedback is the response of the system to a perturbation, usually the change in surface temperature ΔT_s.

Aerosol–cloud interactions (ACIs) are the largest uncertainty in current estimates of anthropogenic radiative forcing of climate (Boucher et al. 2013). Aerosols affect the number concentration of cloud drops N_c, thus altering the brightness (albedo) of clouds (Twomey 1977). Aerosols may alter cloud lifetime as fewer precipitation drops form (Albrecht 1989) and increase liquid water path (LWP).

Cloud feedbacks can be expressed as the change in cloud radiative effects (CREs) divided by the global mean surface temperature change ($\mathrm{W\,m^{-2}\,K^{-1}}$) (Cess et al. 1990). Because CRE is defined as the difference in top-of-atmosphere all-sky and clear-sky radiative fluxes, its change is affected by changes in surface properties or atmospheric composition (Soden et al. 2008). Corrections for these noncloud changes should be applied to accurately assess cloud feedbacks. This can be done using radiative kernels (Soden et al. 2008), known as a

[a] The National Center for Atmospheric Research is sponsored by the National Science Foundation.

Corresponding author address: A. Gettelman, National Center for Atmospheric Research, 3090 Center Green Dr., Boulder, CO 80301.
E-mail: andrew@ucar.edu

DOI: 10.1175/JCLI-D-16-0151.1

kernel-adjusted radiative feedback. Gettelman et al. (2012a) explain this approach using kernels from Shell et al. (2008) and Soden et al. (2008). Dessler (2010) discussed the application of the method to try to tease out climate feedbacks from observations, following Schneider (1972) and Forster and Gregory (2006). The kernel approach has been adapted to directly account for clouds by Zelinka et al. (2012). Cloud feedbacks play a central role in uncertainty surrounding climate sensitivity (Bony et al. 2015; Fasullo et al. 2015).

Several assumptions are commonly made about climate feedbacks. The first assumption is that feedbacks are not a strong function of the climate state or the perturbation from present-day climate. This assumption is distinct from complexities using different methods, particularly with small perturbations (Klocke et al. 2013). Jonko et al. (2012) tested this hypothesis and found weak nonlinearity for moderate radiative forcing. Knutti and Rugenstein (2015) note that such nonlinearity may contribute to spread in estimates across models.

Second, it is generally assumed that feedbacks have low internal variability in any given model, even locally (Armour et al. 2013), and will not vary across different realizations. This has not been tested with single model ensembles.

Aerosols may be important for climate feedbacks as well as for climate forcing. Because ACI alter the mean state of clouds (LWP and N_c), ACI may also alter cloud feedbacks. A cloud with high LWP and small drop concentration could have the same CRE as a cloud with low LWP and high drop concentration, but these clouds may respond differently (different ΔCRE) to a change in surface temperature, giving a different cloud feedback. Thus, an ''aerosol feedback'' may exist such that environmental changes affect aerosol burdens and then the aerosol changes will alter CRE by changing ACI. In this manuscript we will explore these interactions, along with the variance (or internal variability) of climate feedbacks in ensembles of climate simulations from a single model.

These potential modifiers to cloud feedbacks by aerosols are important because the suite of models used for assessments of climate change contains a diversity of approaches and complexity of ACI (Boucher et al. 2013). The extent to which aerosols, and not cloud processes, are contributing to the spread of cloud feedback needs to be assessed as more climate models are including ACI. ACI are usually assessed and quantified by the change in CRE (Gettelman 2015; Ghan et al. 2013); see the definition in section 2.

Several hypotheses will be tested using the same methods, taking advantage of several different ensembles of simulations with a single model (section 2). This extends recent work on multimodel ensembles reviewed by Fasullo et al. (2015). First, we will explore the hypothesis that feedbacks are independent of climate state by investigating feedbacks using two different radiative forcing scenarios with different levels of warming (section 3). Second, each of these ensembles enables us to estimate the spatial variance of the feedbacks across the ensemble members due to internal variability (section 3) in a single model. There have been many analyses of the spread of cloud feedbacks across models (Flato et al. 2013), but no analysis of the spread within a single model ensemble. Third, we will explore how the background state of clouds affects cloud feedbacks and climate sensitivity (section 4). We will compare cloud feedbacks in two different ensembles with the same greenhouse gas forcing but different levels of forcing due to anthropogenic aerosol emissions. This requires a method to control for different ACI between simulations. We also explore analogous climate states and feedbacks in simpler aquaplanet simulations.

This paper builds on previous work to test the extent to which climate feedbacks are similar for different levels of greenhouse gas forcing (Jonko et al. 2012; Klocke et al. 2013). While Klocke et al. (2013) looked at variance due to short-term climate variability, this work presents new analysis on the variance of climate states across ensemble members over long time periods. We also develop a new approach to removing aerosol effects from simulations with interactive aerosols and illustrate the extent to which cloud state affects cloud feedbacks.

Finally, interactive aerosols allow changes to the aerosol distribution induced by changes to climate. The aerosol changes then alter the cloud radiative effect. This is not an aerosol forcing, because it is internal to the climate system. It is rather an aerosol feedback on clouds and climate (section 5). The feedbacks will occur as a result of 1) changes in emissions of natural aerosols into the atmosphere, such as changes to sea salt (a function of surface wind speed over the oceans) or dust (a function of wind speed and soil moisture), 2) changes in scavenging and the lifetime of aerosols resulting from changes in clouds, and/or 3) changes in aerosol direct optical properties resulting from different ambient humidity. We will use the simulations to isolate and quantify this effect. A discussion and conclusions are in section 6.

2. Methods

a. *Feedback methodology*

To determine climate radiative feedbacks, we employ the method of radiative kernels developed by Soden

et al. (2008). The method uses offline kernels that estimate a climate response $\partial R/\partial X$, where R is the shortwave or longwave top-of-atmosphere (TOA) radiative flux in response to a perturbation in state X, where X is temperature, water vapor, clouds, or surface albedo. The feedback is then $(\partial R/\partial X)(\Delta X/\Delta T_s)$, where $\Delta X/\Delta T_s$ is the global annual average surface temperature change derived from the difference of two simulations. Kernels for single-level quantities such as surface albedo and surface temperature are monthly 2D (i.e., latitude by longitude) fields, while temperature and water vapor kernels are 3D (i.e., latitude by longitude by vertical level) monthly fields (Soden et al. 2008). Cloud feedbacks are estimated by the kernel-adjusted CRE, where the kernel adjustments account for changes in the state of water vapor, temperature, and surface albedo that may affect R, and $\mathrm{CRE} = R - R_{\mathrm{clear}}$, where R_{clear} is the clear-sky TOA flux. We also include adjustments for aerosol forcing (see below). Fluxes are calculated separately for the longwave (LW) and shortwave (SW) radiation bands.

The cloud feedback [i.e., $(\partial R/\partial C)(\Delta C/\Delta T_s)$] cannot be directly computed because of the intricate links among clouds, radiation, and the environment. Following Soden et al. (2008) and Shell et al. (2008), the cloud feedback (CF) is the change in CRE divided by the change in surface temperature:

$$\mathrm{CF} = \Delta\mathrm{CRE}/\Delta T_s. \tag{1}$$

The feedback is adjusted by removing terms for changes to water vapor Q, surface albedo α and temperature T in the clear sky c and all sky to get the kernel adjustments to CRE, $\Delta\mathrm{CRE}_k$:

$$\Delta\mathrm{CRE}_k = (K_T - K_T^c)dT + (K_Q - K_Q^c)dQ + (K_\alpha - K_\alpha^c)d\alpha, \tag{2}$$

where K_X is the all-sky kernel and K_X^c is the clear-sky kernel for $X = T$, Q, and α. This yields the kernel-adjusted cloud feedback CF_a:

$$\mathrm{CF}_a = (\Delta\mathrm{CRE} - \Delta\mathrm{CRE}_k)/\Delta T_s. \tag{3}$$

Traditionally radiative kernels are run on equilibrium experiments, but regression methods (Gregory et al. 2004) and comparison tests (Gettelman et al. 2012a) indicate that flux imbalances can be included as part of the forcing [see also discussion by Medeiros et al. (2015)]. The use of models with TOA flux imbalances allows application of the kernels to transient experiments. In equilibrium, the model used here does not have an imbalance.

The method follows the work of Gettelman et al. (2012a) and Gettelman et al. (2013), who illustrated the causes of the change in climate sensitivity between different versions of the Community Earth System Model (CESM). The kernels were originally developed by Shell et al. (2008) for version 3 of the Community Atmosphere Model (CAM), but in general the kernels are stable across models (Soden et al. 2008). The code has been updated to run on output from the current version of CESM (CESM1.1). We do not use the cloud property kernels developed by Zelinka et al. (2012) because the necessary simulator outputs were not available from the CESM experiments used (see below).

b. Aerosol kernel adjustment

One of the complexities of estimating feedbacks using these transient simulations with different aerosols is that ACI alter CRE. This additional dimension to the feedbacks may affect the ''efficacy'' (efficiency) of different climate forcings (Hansen et al. 2005). To remove the aerosol forcing effect, we will calculate an ''aerosol kernel'' to adjust the cloud forcing for the direct and indirect effect of aerosols (mostly indirect).

Following Eq. (2) above we add a term for the aerosol kernel:

$$\Delta\mathrm{CRE}_k = (K_T - K_T^c)dT + (K_Q - K_Q^c)dQ + (K_\alpha - K_\alpha^c)d\alpha + (K_A - K_A^c)dA, \tag{4}$$

where A is aerosols, and dA is ΔAOD, the change in aerosol optical depth (AOD). The aerosol kernel for all sky K_A and clear sky K_A^c is estimated from

$$K_A = \partial R/\partial\mathrm{AOD} \tag{5}$$

and

$$K_A^c = \partial R_c/\partial\mathrm{AOD}, \tag{6}$$

where ∂R is the change in all-sky flux and ∂R_c is the change in clear-sky flux due to aerosols. The aerosol kernel is approximated based on a difference of two simulations as $\Delta R/\Delta$AOD and $\Delta R_c/\Delta$AOD at each horizontal location (x, y): the change in TOA radiation ΔR, occurring because of the change in aerosols ΔAOD. The aerosol kernel is similar to the other kernels in that it is a TOA radiative response to a difference to a perturbation to the system. It is similar to the surface albedo kernel as a response to a single-level (column) perturbation. The aerosol kernel is different in that it is not estimated from a unit perturbation, but rather from another set of model simulations.

The kernel is applied to remove flux perturbations, similar to how other kernels (such as surface albedo) are applied to generate kernel-adjusted cloud feedbacks. All adjustments, including aerosols, are made at the

same time. As with the other kernels, both clear- and all-sky kernels are applied. The clear-sky aerosol kernel is basically the direct effect and all-sky kernels are the total effect (mostly the cloud effect). The effects shown in sections 4 and 5 are with aerosol kernels applied with all other adjustments. For example, a change in surface albedo will affect the clear-sky TOA flux, which is aliased into the cloud radiative effects. The adjustment for surface albedo takes the α change $\Delta\alpha$ between two simulations, and multiplies this by the surface albedo kernel $\partial R/\partial\alpha$ at each point to remove this ΔR from ΔCRE [Eqs. (2) and (4)]. Aerosols cause clouds to be brighter because of a change in drop number (and potentially cloud lifetime). The aerosol kernel adjustment uses ΔAOD multiplied by the aerosol kernel $K_A = \Delta R/\Delta\text{AOD}$ to estimate an additional ΔR to remove from ΔCRE [Eq. (2)]. This is done for K_A and K_A^c in the LW and SW radiation.

Because it uses a difference between two simulations, for stability a threshold of $\Delta\text{AOD} > 0.01$ locally is applied. This means that clean regions do not see aerosol perturbations. Regions where the aerosol kernels are applied are inside the filled contour in Fig. 1, meaning most of the Northern Hemisphere. The clean regions ($\Delta\text{AOD} < 0.01$) are mostly only over the poles and the Southern Hemisphere oceans. However, they also do not see large TOA flux perturbations due to aerosols (e.g., Gettelman 2015, his Fig. 8). The results (and conclusions) are not very sensitive to the AOD threshold.

Estimating the aerosol kernel is dependent on the particular climate model formulation and aerosol distribution. The aerosol kernel is not strongly dependent on the climate state (see below). The stability is expected given the magnitude of the kernel forcing (locally $10\,\text{W}\,\text{m}^{-2}$) and the dominance of the effect in the shortwave radiation, while the greenhouse gas forcing alters the climate state by the longwave emission of CO_2 and H_2O, modulated by clouds.

Fortunately, our methodology and ensembles will minimize these uncertainties. We are using the same model [CESM1(CAM5)] for all simulations. Furthermore, we will estimate the kernel using a similar pattern of ΔAOD, and an appropriate range of ΔAOD that brackets the emissions changes in the ensembles. Accordingly, the aerosol kernel is calculated from two 50-yr CAM5 simulations with 2000 and 1850 aerosol emissions. For a 50-yr simulation, the local standard deviation in annual TOA flux in the Northern Hemisphere storm track is approximately $3\,\text{W}\,\text{m}^{-2}$. Using a 95% confidence Student's t test, this means local (not global) deviations of larger than $0.7\,\text{W}\,\text{m}^{-2}$ are statistically significant, and the regions of the aerosol kernel meet this criterion (e.g., Gettelman and Morrison 2015, their Fig. 8). These are not idealized kernels; they are estimated from a similar perturbation as the one we are trying to remove, and using the same model physics. Regions of high aerosol susceptibility but no change in aerosols have a small aerosol kernel correction. This limits the analysis to regions with significant aerosol perturbations based on current distributions of aerosols. In the case of these ensembles of model runs, these are exactly the perturbations we are testing. We have also tested the sensitivity of the kernel by repeating the analysis using alternative kernels from 1) a different model configuration and 2) the same configuration but with a climate reflecting the end of the representative concentration pathway 8.5 (RCP8.5) climate of a warmer planet with higher (doubled) CO_2. Perturbations to the aerosol kernel are discussed in section 4.

Figure 1 illustrates the kernels [K_A in Eq. (5) and K_A^c in Eq. (6)] for clear-sky SW (Fig. 1a), all-sky SW (Fig. 1b), clear-sky LW (Fig. 1c), and all-sky LW (Fig. 1d) radiation. Kernels are estimated monthly, while annual means are shown in the figures. Note that the scale is different for each clear-sky panel. The all-sky kernels are larger (representing cloud effects and ACI) with the SW kernels being the largest (Fig. 1b). Note that a typical local AOD change in the Northern Hemisphere is on the order of 0.02–0.03, so this implies changes locally of several watts per square meter. The kernel reflects the changes in the emissions between preindustrial and present because the changes to top-of-atmosphere flux ΔR tend to be regionally constrained to regions near where aerosols are changing ($\Delta\text{AOD} > 0.01$). The annual mean $\Delta\text{AOD} < 0.01$ line is shown on each panel in Fig. 1. It also illustrates that this is not a unit perturbation (perturbing AOD by 0.01 and then estimating the response) since the effects are not simple direct radiative calculations but rather involve nonlinear ACI effects on clouds. In regions over the oceans far from aerosol sources, there is little effect of the aerosol kernel. There may still be susceptibility of clouds to ACI in these clean regions, but it is not seen with these aerosol perturbations. However, the kernels do agree well with the top-of-atmosphere flux differences in the simulation from which they were generated. The aerosol kernel is thus model and perturbation specific.

We illustrate the effect of applying this kernel in section 4 and show that it is effective at removing aerosol effects. As noted by Hansen et al. (2005) and Shindell (2014), the efficiency (or efficacy) of different forcings such as aerosols may be different than CO_2. But for effective radiative forcing (ERF) where the troposphere adjusts, aerosol forcing has an efficacy close to unity (Hansen et al. 2005; Marvel et al. 2015).

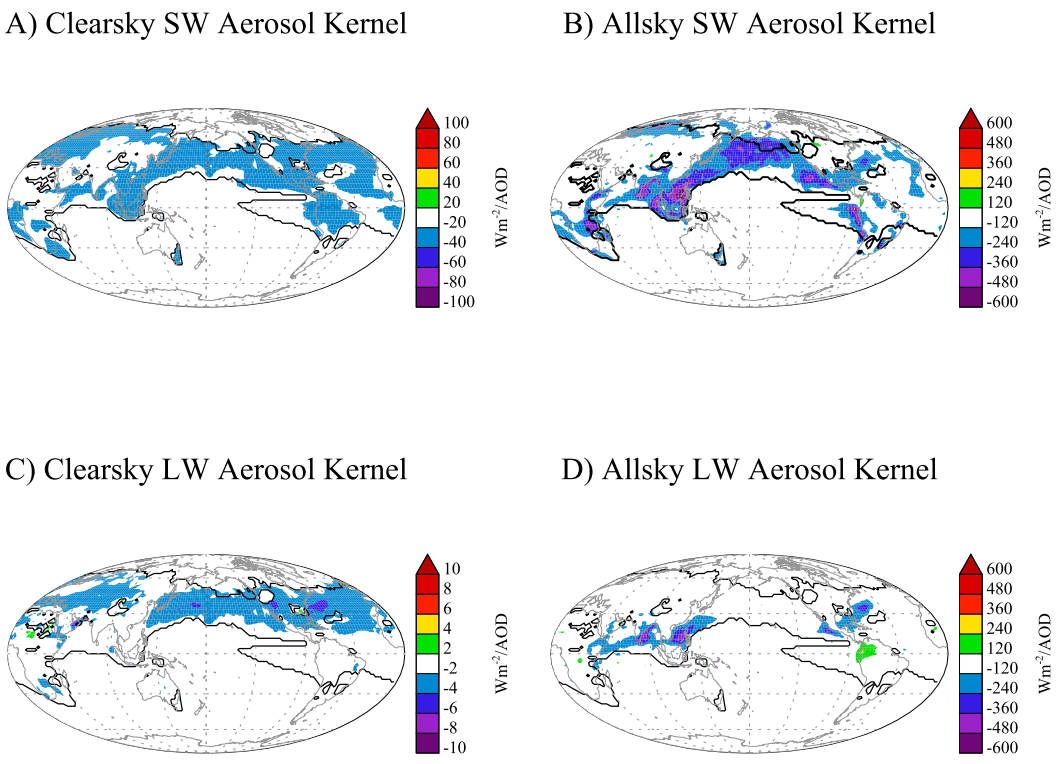

FIG. 1. Maps of annual mean K_A (W m^{-2} per unit AOD): (a) clear-sky SW, (b) all-sky SW, (c) clear-sky LW, and (d) all-sky LW radiation. Black contour indicates the annual mean value of ΔAOD = 0.01 (see text).

c. *Models*

All experiments use CESM1 simulations, with the Community Atmosphere Model, version 5 (CAM5; Neale et al. 2010). CESM1(CAM5) includes a modal aerosol model (Liu et al. 2012) in the atmosphere with prognostic aerosols, and physically calculated ACI in the stratiform cloud regime (Gettelman et al. 2010).

1) ENSEMBLES OF COUPLED SIMULATIONS

The CESM Large Ensemble (CESM-LE, or LE) of 30 members is described by Kay et al. (2014b). The CESM-LE follows a RCP emission scenario for greenhouse gases (GHGs) and aerosols with 8.5 W m^{-2} of forcing in 2100 (van Vuuren et al. 2011). We also use a CESM Medium Ensemble (CESM-ME, or ME) described by Sanderson et al. (2016). The CESM-ME has 15 ensemble members that use RCP4.5 with 4.5 W m^{-2} of forcing in 2100 (van Vuuren et al. 2011). We also use the CESM Fixed Aerosol Ensemble (CESM-FixA, or FixA). As described by Xu et al. (2016), the FixA ensemble has 15 members and uses the same RCP8.5 scenario as the LE, but the FixA ensemble fixes aerosol emissions at constant year 2005 values starting from year 2006. The ensembles for ME and FixA were run to 2080. All versions use the same model code for CESM. The only differences are the GHG and aerosol forcing.

2) AQUAPLANET EXPERIMENTS

To aid in the interpretation of the ensembles, we also turn to simpler experiments using an aquaplanet configuration of CESM (Medeiros et al. 2016). This version uses fixed sea surface temperatures, and the same physical parameterizations as in the CESM ensembles. To simulate climate changes, we run CESM-Aqua with a control case, and a case with doubled carbon dioxide (367–734 ppm) and a uniform increase in SST of +4 K. This is a standard test for producing feedback estimates from aquaplanet simulations.

To test the sensitivity to aerosols, pairs of experiments are conducted with different fixed N_c: 50, 100, and 300 cm^{-3} with double-moment microphysics. This is done so that tests can be performed without aerosols (which have a land and ocean contrast), but to mimic the effects of aerosols. The range is chosen to mimic the effect of anthropogenic aerosols on top of atmosphere fluxes (see below). A value of N_c = 100 cm^{-3} is the baseline, while N_c = 50 cm^{-3} is typical of marine conditions and N_c = 300 cm^{-3} is more typical of continental or polluted conditions. These simulations are called

Nc100, Nc50, and Nc300, respectively. The different drop numbers result in differences in the SW CRE in the control case. The net global SW CRE in the aquaplanet control simulations is −60.6, −64.3, and −70.0 W m^{-2} for simulations Nc50, Nc100, and Nc300 respectively. To isolate the difference of N_c in the base state, an additional simulation was conducted where the base state in the Nc300 simulation was adjusted back to a SW CRE similar to that in the Nc50 simulation. The adjustment was accomplished by reducing the cloud fraction, through an increase in the critical relative humidity for cloud formation in the cloud macrophysics (Park 2014). The change does not alter the pattern of cloud forcing appreciably, only its magnitude. This simulation, called Nc300RH, has a global-mean base state SW CRE of −61.4 W m^{-2}, close to the Nc50 case. The difference in top-of-atmosphere flux between the Nc300 and Nc50 cases is −2.2 W m^{-2}, which is similar to the −1.5 W m^{-2} change due to anthropogenic aerosols in the full model calculation.

d. Hypotheses

The different hypotheses to be tested and the methods of using these ensembles to test them are outlined below.

1) Feedback variance

We hypothesize that kernel-adjusted fast feedbacks have small variability on a global basis across ensemble members (internal variability), but may have large local variability. This hypothesis can be tested by estimating feedbacks from a 100-yr section of the CESM-LE control and 20 years of each ensemble member at the end of the twenty-first century (2060–80). We seek to quantify the variance across the ensemble members of each feedback and to understand the patterns of variance and how it varies. We will examine the sensitivity to the number of members or the years averaged.

2) Feedback linearity

Second, we wish to test if feedbacks are constant between different ensembles. The forcing and surface temperature changes are different between the ME (RCP4.5) and the LE (RCP8.5) simulations. But the feedbacks are normalized by ΔT_s. To understand if the different feedbacks are the same we will estimate and compare kernel-adjusted feedbacks from each ensemble (average and spread).

3) Aerosol effects

Third, we hypothesize that aerosols will alter cloud state (LWP and N_c), and a different cloud state may affect climate feedbacks. To test this hypothesis, we will calculate feedbacks for the FixA simulation (constant aerosol forcing case) to determine if they are different than for the LE (RCP8.5). The surface temperature will be different. The FixA simulation has higher cloud drop number concentrations, particularly in the Northern Hemisphere, as a result of anthropogenic aerosols. It will warm and less than the LE simulation, because of the continuation of aerosol radiative forcing due to both direct and indirect effects of aerosols. If the feedbacks are not dependent on the degree of warming (tested by comparing LE and ME with similar aerosols as noted above), then any feedback differences between FixA and LE simulations should be due to aerosols. To understand the effects, we analyze the cloud state (mean column drop number, LWP, etc.) in the LE simulation and the FixA ensemble. The difficulty is that there are differences in patterns of the aerosol emissions over time. We use aerosol kernels to control for changing aerosol radiative effects.

4) Aerosol feedbacks

Finally, with interactive aerosols, there can be changes to the aerosol distribution induced by changes to climate. We will test the hypothesis that climate-induced aerosol changes can alter CRE. This is not an aerosol forcing, because it is internal to the climate system. It is rather an aerosol feedback on clouds and climate. As with aerosol radiative forcing, these effects can be both direct and indirect. As noted above, there are several possible internal mechanisms that can change aerosol populations to create this feedback.

e. Aerosols in CESM

To test these hypotheses we perform several analyses. First, we estimate feedbacks based on a 100-yr section of the CESM-LE control, and then 20 years of each CESM-LE member in the late twenty-first century (2080–60). So feedbacks are 2060–80 minus the control (1850 forcing). Note that between 1850 and 2060, anthropogenic aerosols first rise and then fall again, so that past and future periods have similar but not identical aerosols. CESM-LE uses RCP8.5 with increased greenhouse gases and reduced aerosols in the twenty-first century.

We do the same for the CESM-ME (RCP4.5) ensemble members. The control simulation for the LE and ME are the same. RCP4.5 has a reduction of aerosols in the future, similar to RCP8.5. Finally we also estimate the feedbacks for each member of the FixA (constant aerosol) ensemble. Since the FixA ensemble was run from 2006 to 2080 with fixed aerosols, we subtract 2006–26 from 2060–80 values. This case has high aerosol loading throughout. Figure 2a illustrates the aerosol loading by latitude for the different simulations and

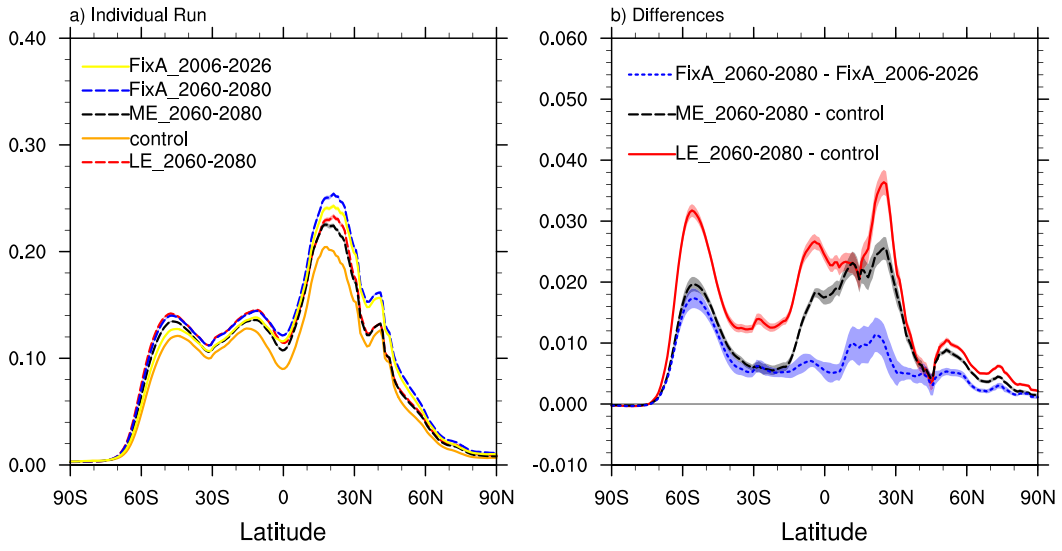

FIG. 2. Zonal-mean (a) AOD at 550-nm wavelength and (b) change in AOD from three ensembles of simulations: LE (red), ME (black), and FixA (blue). Also shown in (a) are the control simulation for ME and LE (orange) and the FixA control (2006–26; yellow). The two standard deviation spreads of zonal-mean AOD across each ensemble are shown by the shaded regions in (b).

periods. Figure 2b shows the change in AOD between the analyzed beginning and end points of each ensemble.

Feedbacks calculated with radiative kernels using 2006–26 (20 yr) as the base period for all three ensembles (LE, ME, and FixA) are qualitatively and quantitatively similar to using the longer control run for ME and LE. The benefit of using the control simulation for LE and ME is to minimize the difference in aerosol loading between time periods. The choice of base period only impacts the standard deviations: using 20 years from different ensembles results in larger feedback spread (by about a factor of 2) than using 100 years of the same control run. This explains much of the difference in standard deviation between FixA and ME simulations, which have more internal variability (larger standard deviation) than LE because of the smaller ensemble size.

Figure 2 illustrates that both the latitudinal distribution of aerosols and the absolute amount are quite different in different time periods. The change in aerosols between different time periods of each ensemble is due to both external changes in emissions and aerosol feedbacks due to climate changes that affect aerosols. In the FixA ensemble, the emissions changes are eliminated and any change in aerosols is due to a climate influence on aerosols (aerosol feedbacks). These feedbacks include changes in winds that influence sea salt emissions (in the Southern Ocean, peaking at 60°S) and changes in tropical dust (one-third of the change at 30°N), as well as internal changes to aerosol transport, scavenging, and optical properties.

The differences in Fig. 2 for the LE and ME simulations arise mostly from the emissions. Lamarque et al. (2011, see their Fig. 9) illustrate that AOD in 2080 is similar between RCP4.5 and RCP8.5 but that it is not the same as AOD in 1850 (used for the control). It is more similar to global AOD in 1950–70. Figure 10 in Lamarque et al. (2011) clearly shows the local SO_4 and black carbon column burdens are not the same because of a shift of aerosols into the tropics. Even if we looked at the same global AOD, there would be differences in AOD patterns, consistent with increased AOD in the tropics, and still some at NH midlatitudes.

To adjust for these different levels and locations of AOD changes, we will use K_A to correct the clear-sky and all-sky radiative forcing for the changes to aerosols diagnosed in these simulations. Furthermore, we will use aquaplanet simulations to understand the global results.

3. Variance results

Table 1 illustrates a summary of climate feedbacks for the different ensembles, and the standard deviation within each ensemble. The feedbacks may differ because of aerosols or climate forcing, and we will try to pull this out of the analysis. A comparison of feedbacks in our Table 1 with those in Table 2 of Gettelman et al.

TABLE 1. Temperature change (ΔT_s; K) and feedback terms ($W\,m^{-2}\,K^{-1}$) for different ensembles. Values in parentheses are the standard deviation across the ensembles. Regional total cloud feedback (total cloud) results are area averaged to be representative of the fraction of the global total. Cloud feedbacks are also shown with three different aerosol kernel adjustments as described in the text.

Ensemble	LE	ME	FixA
ΔT_s	3.47 (0.03)	2.26 (0.03)	2.09 (0.05)
Feedback			
Planck	−2.13 (0.01)	−2.09 (0.01)	−2.13 (0.02)
Lapse rate	−0.49 (0.01)	−0.43 (0.01)	−0.49 (0.02)
H_2O	1.67 (0.01)	1.61 (0.02)	1.65 (0.03)
Albedo	0.32 (0.00)	0.35 (0.01)	0.32 (0.01)
Total cloud	0.18 (0.01)	0.21 (0.01)	0.49 (0.02)
LW cloud	−0.10 (0.01)	0.01 (0.01)	−0.03 (0.01)
SW cloud	0.28 (0.01)	0.20 (0.01)	0.52 (0.03)
Aerosol kernel K_A			
Total cloud	0.41 (0.01)	0.47 (0.01)	0.60 (0.02)
LW cloud	−0.17 (0.01)	−0.03 (0.01)	−0.04 (0.02)
SW cloud	0.58 (0.01)	0.50 (0.02)	0.64 (0.03)
Aerosol kernel alt			
Total cloud	0.25 (0.01)	0.29 (0.01)	0.52 (0.02)
LW cloud	−0.11 (0.01)	0.01 (0.01)	−0.02 (0.02)
SW cloud	0.36 (0.01)	0.28 (0.01)	0.55 (0.03)
Aerosol kernel alt2x			
Total cloud	0.24 (0.01)	0.27 (0.01)	0.51 (0.02)
LW cloud	−0.11 (0.01)	0.02 (0.01)	−0.02 (0.01)
SW cloud	0.35 (0.01)	0.25 (0.01)	0.54 (0.03)
Regional			
Total cloud, 50°–15°S	0.07 (0.01)	0.11 (0.01)	0.13 (0.02)
Total cloud, 15°S–15°N	0.17 (0.01)	0.16 (0.01)	0.24 (0.01)

(2012a) indicates that these transient experiments yield results very similar to traditional slab or mixed layer ocean model feedback experiments, or modified-Cess (see Cess et al. 1990; fixed sea surface temperature) experiments. The model here, CESM1.1.1, is very similar to the CAM5 experiments in Gettelman et al. (2012a), and feedbacks are comparable. Water vapor and lapse rate feedbacks differ by about $0.2\,W\,m^{-2}\,K^{-1}$ between these experiments and those of Gettelman et al. (2012a), but the combination of the two feedbacks is similar ($\sim 1.2\,W\,m^{-2}\,K^{-1}$). Albedo feedback magnitudes are also very similar ($\sim 0.3\,W\,m^{-2}\,K^{-1}$). Aerosol kernels are only applied to cloud feedbacks. The cloud feedbacks with the aerosol kernel applied are also similar to previous versions ($\sim 0.5\,W\,m^{-2}\,K^{-1}$). Two alternative estimates of the aerosol kernel (denoted alt and alt2x) are used to test the sensitivity of the results to the aerosol kernel. The alt kernel uses simulations with a revised version of the cloud microphysics (Gettelman and Morrison 2015) and different cloud tuning. The ACI are slightly lower. The third kernel (alt2x) was also estimated using this same model configuration but with climate conditions (CO_2 concentration and sea surface temperatures) reflecting a doubling of CO_2 (720 ppmv). Next we discuss the variance of feedbacks in more detail.

a. Water vapor feedback variance

Figure 3 illustrates the water vapor feedback from the three ensembles. For this and other zonal mean figures, the feedback is presented in terms of petawatts ($1\,PW = 10^{15}\,W$) per degree of latitude. This essentially weights the feedback by the area of a latitude circle so that the integral represents the global mean value ($W\,m^{-2}$). The figures give a visual picture of where the feedbacks are important in the global mean. The feedback is generally very similar across the ensembles. There is a slight difference in the water vapor feedback between ensembles in the Northern Hemisphere. The differences are partially due to surface temperature: the LE simulation is the warmest, followed by the FixA ensemble (slightly cooler because of aerosols), and the ME simulation has the lowest mean surface temperature (because of reduced radiative forcing in RCP4.5 vs RCP8.5). This is consistent with weak nonlinearities in water vapor feedbacks (Jonko et al. 2012). Regional differences are largely due to dry subtropical regions of the Sahara and western Indian Ocean. The ensemble spread and standard deviation are quite small, only a few percent of the value, and the differences in the Northern Hemisphere subtropics are small. Global totals of feedback terms from each ensemble are in Table 1, and the water vapor feedback is very similar, with the small difference following the zonal difference in the NH subtropics in Fig. 3. There is no discernible pattern in the horizontal distribution of feedback variance. Variance is higher in the FixA ensemble than the ME or LE simulations, although the global integral is quite small. This is due to the difference in base period (there is only a single control simulation, and it is 100 years long). For LE and ME simulation feedbacks estimated with a 20-yr base period of 2006–26 (the same as FixA), variance is comparable across ensembles.

b. Albedo feedback variance

Zonal-mean surface albedo feedbacks are illustrated in Fig. 4. Given the large variance in high-latitude climate, as seen for example in high-latitude surface air temperature trends in Kay et al. (2014b) for the LE simulations, it might be expected that snow- and ice-covered surfaces will exhibit more variance. In Fig. 4, there is little variance or difference between the ensembles in the Southern Hemisphere. However, there is a difference between the ensembles in the Northern Hemisphere, and larger variance for the FixA ensemble. The largest variance occurs at the sea ice edge near

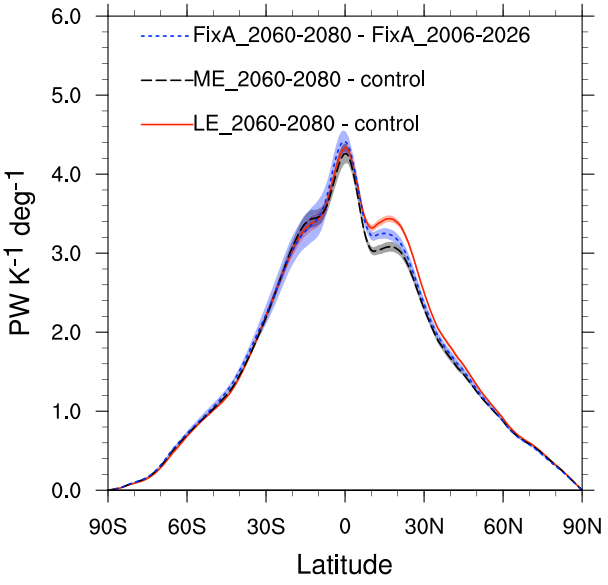

FIG. 3. Zonal-mean vertically integrated water vapor feedback [PW K^{-1} (° lat)$^{-1}$] from three ensemble simulations: LE (red solid), ME (black dashed), and FixA (blue dotted). The two standard deviation spreads of zonal mean feedback across each ensemble are shown by the shaded regions.

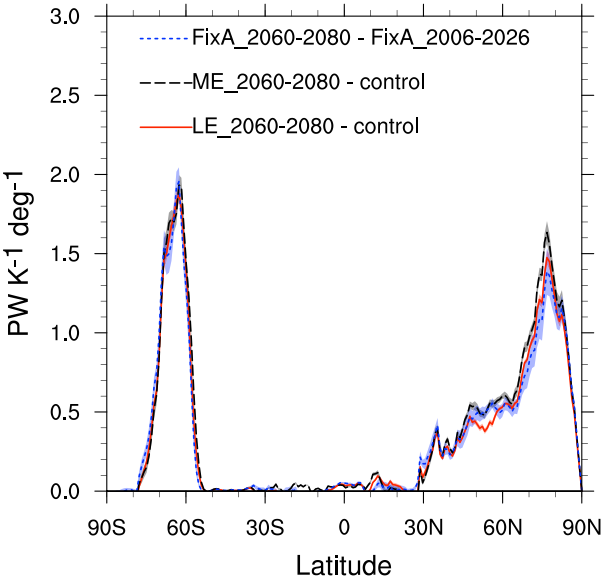

FIG. 4. As in Fig. 3, but for zonal mean albedo feedback.

70°N, and is regionally similar across ensembles. Variance locally reaches only 10%–20% of the mean value. The albedo feedback variance is larger in the FixA ensemble because the FixA ensemble feedbacks are estimated using two 20-yr periods, while the ME and LE simulations use 100 years of the control simulation. As a result, the variance doubles (Table 1). As with the water vapor feedback, we verified that the variance goes down when feedbacks are estimated for the FixA ensemble using the 100-yr control, and they go up for the LE simulation when using a 20-yr control.

c. *Cloud feedback variance*

Figure 5 illustrates the zonal-mean adjusted cloud feedbacks from the different ensembles, following Eq. (2) and *not* including the aerosol kernel. The differences in cloud feedbacks between the LE and the ME, with different ΔT_s are small (Fig. 5), indicating that the level of warming does not really matter and the cloud feedback is constant with forcing in this range. However, it is clear that the cloud feedback structure is quite different in the FixA simulation, which we will discuss in the next section. The variance in cloud feedbacks is small in the zonal mean, and regionally (see below). As with albedo feedbacks, the cloud feedback variance is larger in the FixA ensemble because the FixA ensemble feedbacks are estimated using two 20-yr periods with variability in both, while the ME and LE simulations use 100 years of the control simulation for the base period, with only a single control. For the FixA simulation, variance maximizes in the eastern subtropical oceans at about 25% of the mean value (not shown).

d. *Variance summary*

For all the feedbacks examined, different ensemble members may differ on short-term trends, but they do not differ on long-term feedbacks, even when those feedbacks are estimated from only 20 years of a transient climatology (Table 1). Feedback variance is larger if only 20 years of the control are used (rather than 100 years), but it is still a small fraction of the global feedback (Table 1), even regionally (in the zonal mean, Fig. 5).

This is true of water vapor (Fig. 3), cloud (Fig. 5), and albedo (Fig. 4) feedbacks. The water vapor and albedo feedbacks across the ensembles are very similar: they are not dependent on the degree of warming, or on the level of aerosols in the simulations. Cloud feedbacks are similar between the LE (RCP8.5) and ME (RCP4.5) simulations. The cloud feedbacks differ with aerosol loading, and need to be corrected for changing aerosol forcing, the subject of the next section.

4. Results: Aerosol influence on cloud feedbacks

Figure 5 indicates that simulations with different aerosol loading have important differences in cloud feedbacks. However, the different aerosol loadings create different forcing, and we now use the aerosol kernel, following Eq. (4), to separate changes in ACI (forcing) from cloud feedbacks and remove aerosol forcing from cloud feedbacks in Fig. 6.

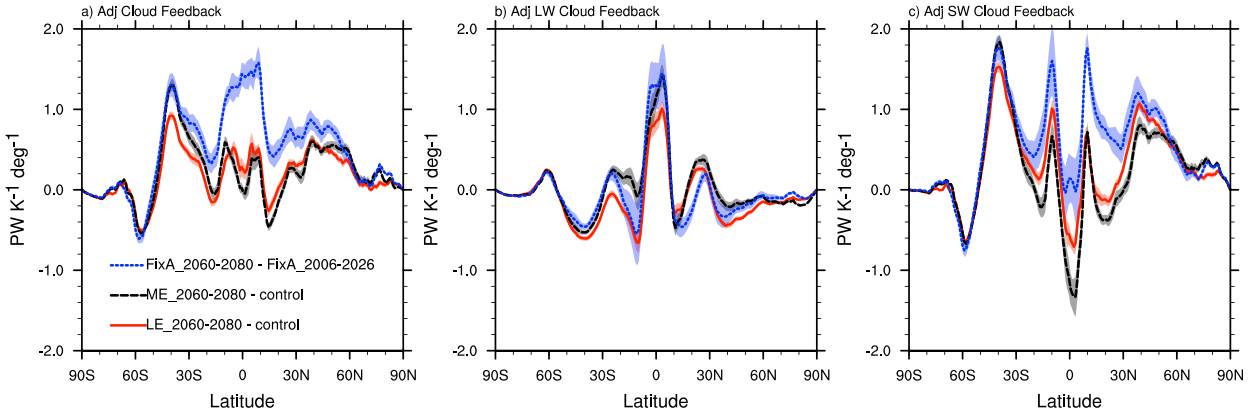

FIG. 5. Zonal-mean (a) total (LW + SW), (b) LW, and (c) SW kernel-adjusted cloud feedback [PW K^{-1} (° lat)$^{-1}$] from three ensemble simulations (aerosol kernel not included): LE (red solid), ME (black dashed), and FixA (blue dotted). The two standard deviation spreads of zonal mean feedback across each ensemble are shown by the shaded regions.

The adjustment brings the cloud feedbacks between the simulations into better agreement (Fig. 6), particularly in the Northern Hemisphere midlatitudes and in the tropics where aerosol changes in the ME and LE simulations would be aliased into the cloud feedbacks. In general the cloud feedbacks are more positive when adjusted for aerosol changes. In the LE and ME simulations the future has higher aerosols than the preindustrial control simulation (Fig. 2). The aerosol kernel removes this cooling effect, making ΔCRE and feedbacks more positive. The FixA ensemble has less of a correction because aerosol emissions are constant. The effects come from both the longwave and shortwave radiation, implicating cold clouds (high- and midlevel clouds) in the tropics and low-level clouds in the subtropics.

Table 1 illustrates results with two different aerosol kernels to assess sensitivity of the results to the aerosol kernel. Lower ACI in the alt kernel using a simulation with different cloud microphysics result in a reduced correction of the cloud feedbacks compared to the standard kernel, but the differences between FixA ensemble and LE or ME simulation remain for any kernel. Furthermore, there is basically no difference between results using the alt2x kernels estimated with a high CO_2 climate (warmer world) or the standard kernel for the present, so the aerosol kernels will not be different for future climates.

The FixA simulation falls between the LE and ME simulations in ΔT_s, but has different cloud feedbacks. Cloud feedbacks are significantly more positive in the FixA simulation (Fig. 6 and Table 1). The higher cloud feedbacks occur mostly in the tropics and subtropics. In the tropics, the differences in cloud feedback between FixA ensemble and LE or ME simulation (Fig. 6) account for a difference in total cloud feedbacks of 0.07–0.08 W m^{-2} K^{-1}, or about 15%–20% of the total cloud feedback. It is significantly larger than the internal variability of cloud feedbacks (one standard deviation of 0.02 W m^{-2}).

Figure 7 illustrates the location of the feedback differences. The FixA simulation has stronger positive

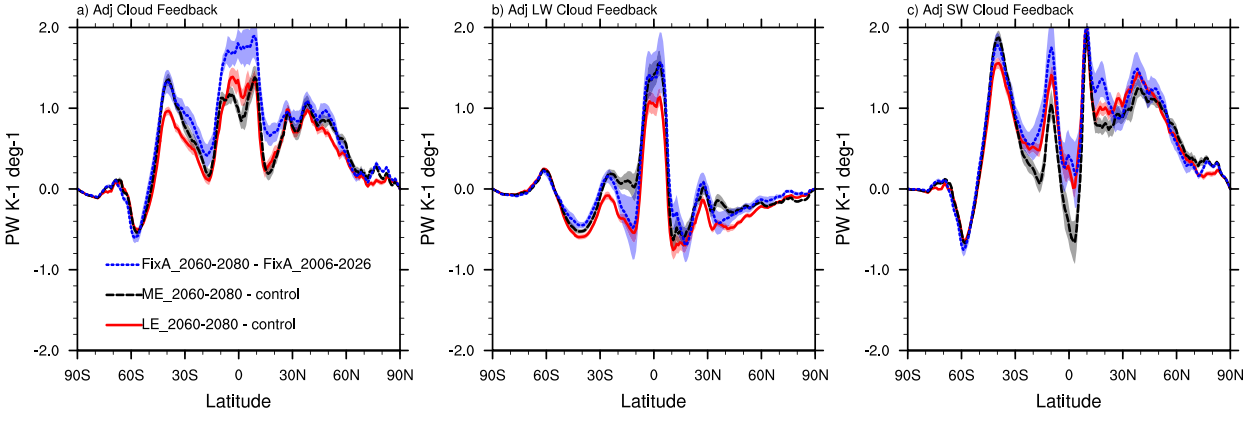

FIG. 6. As in Fig. 5, but for kernel-adjusted cloud feedback, including aerosol kernels.

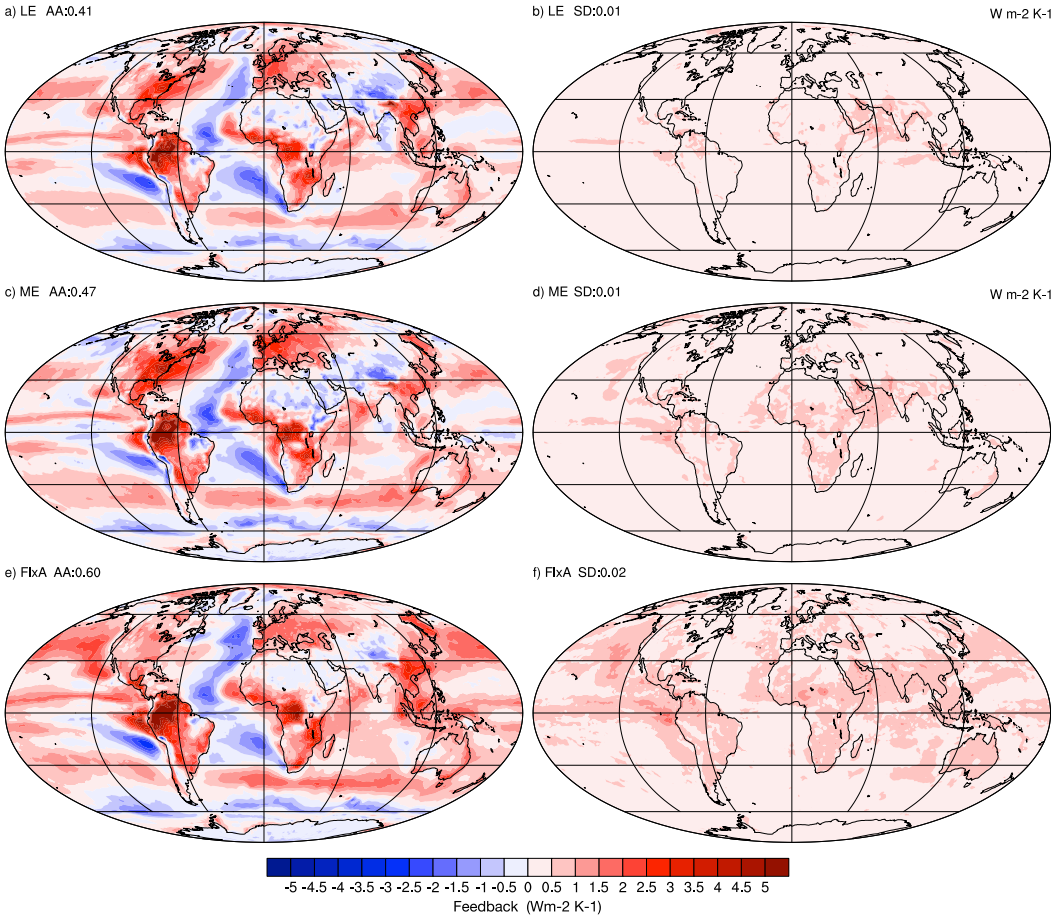

FIG. 7. Maps of total (LW + SW) kernel-adjusted cloud feedback ($\mathrm{W\,m^{-2}\,K^{-1}}$) from three ensemble simulations with aerosol kernel applied: (a),(b) LE, (c),(d) ME, and (e),(f) FixA. Local standard deviations of the adjusted cloud feedback across each ensemble are shown in (b),(d), and (f).

feedbacks in the Northern Hemisphere Pacific storm track, with weaker feedbacks over land. Tropical feedbacks are also stronger in the eastern Pacific and over the Maritime Continent. These are close to regions where the aerosols most affect clouds (Fig. 1). The increase in positive feedbacks in the tropics is mostly from the LW radiation, and seems mostly related to regions with high clouds. This is consistent with positive increases in cloud radiative forcing from anthropogenic aerosols that increase homogeneous freezing with higher sulfate loading (Gettelman et al. 2012b). It may also be that the higher aerosol loading is still affecting the high clouds in ways not fully reflected in the aerosol kernel. These might be related to warmer climates with larger forcing changes than that induced in present climates. We will explore this idea further below.

Figure 8 presents tropical cloud feedbacks from the different ensembles sorted by dynamical regime based on the 500-hPa vertical velocity. Following Bony and Dufresne (2005), we composite cloud feedbacks for all points based on the base case 500-hPa pressure velocity ω_{500}. The results show a characteristic pattern of positive LW radiative feedbacks in tropical convective regimes with upward motion (large negative ω_{500}), and largest positive SW radiative feedbacks in regions with weak subsidence ($0 < \omega_{500} < 20\,\mathrm{hPa\,day^{-1}}$). The FixA ensemble has higher positive net feedbacks because of more positive feedbacks in both regimes.

Aquaplanet

To analyze the possible effect of aerosols on cloud feedbacks, aquaplanet simulations were conducted with different specified drop number concentrations. Three different specified N_c were explored: $N_c = 50$, 100, and $300\,\mathrm{cm^{-3}}$. An additional experiment to adjust the cloud forcing (Nc300RH) was also conducted (see section 2). Experiments are the difference between Control and SST + 4 K perturbation simulations. Adjusted cloud

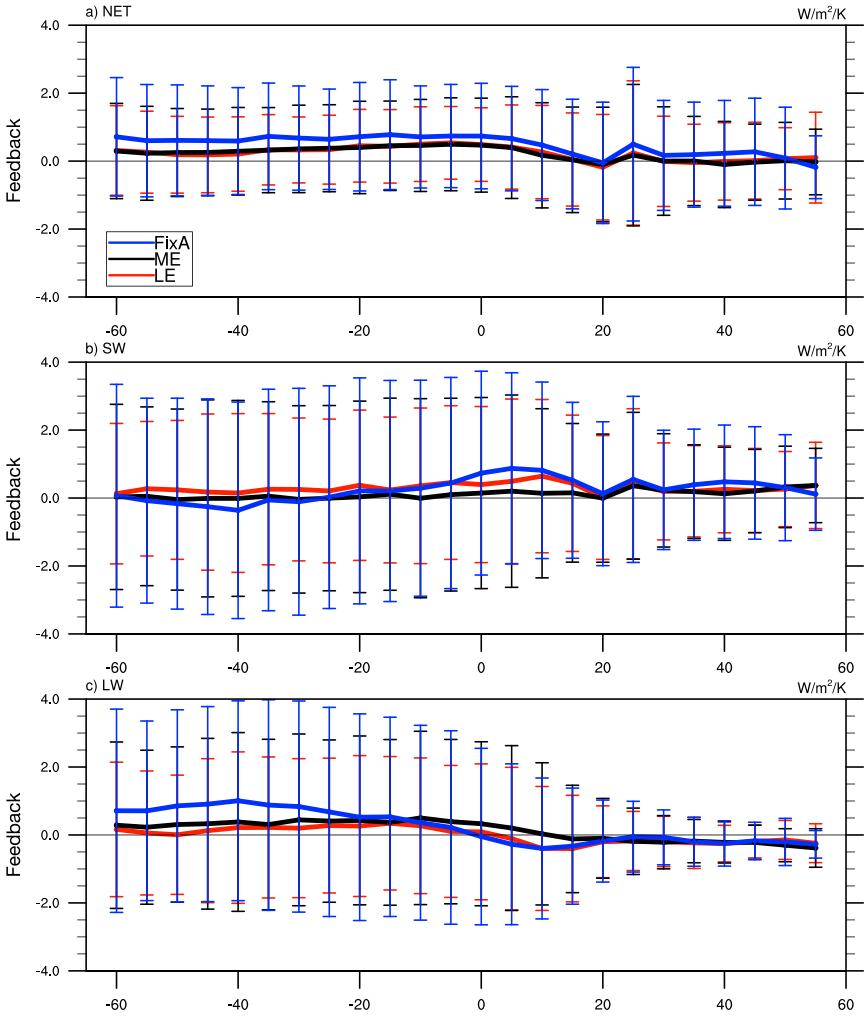

FIG. 8. Tropical (30°S–30°N) (a) net, (b) SW, and (c) LW radiation kernel-adjusted cloud feedback (with aerosol kernel applied; $W\,m^{-2}\,K^{-1}$) composited by 500-hPa level vertical (pressure) velocity ($hPa\,day^{-1}$). Error bars are two standard deviations in each bin. A single ensemble member is used from FixA (blue), ME (black), and LE (red) simulations.

feedbacks are shown in Fig. 9. Since the aquaplanet configuration is symmetric about the equator the hemispheres are averaged together.

The structure of the feedbacks is different than in a standard (Earth-like) simulation. This is due to the different aquaplanet climate regimes. The convective regions are a single intertropical convergence zone (ITCZ) band in each hemisphere at 5° latitude, with a narrow region along the equator that looks like a stratocumulus regime. The subtropical dry regions peak at about 20° latitude, and the storm tracks start poleward of this, peaking at 45° and ending by 60° latitude. Cloud feedbacks in the region from 45° to 60° latitude are qualitatively similar to cloud feedbacks in midlatitudes of the full simulation (Fig. 6), but the tropics are different.

The peak in cloud feedbacks at 10°–20° latitude (Fig. 9a) comes mostly from the LW cloud feedbacks (Fig. 9b). This occurs in the subtropical dry regions in the aquaplanet: in effect the overturning Hadley circulation is compensating for the lack of zonally asymmetric Walker circulation in the full model, which allows changes in high clouds in the tropics. These feedbacks get more positive with increasing liquid drop number, likely due to higher LWP in the simulations with higher drop number, but that also occurs for the Nc300RH case in which LWP is reduced. Nc300 and Nc100 have larger magnitude of cloud feedbacks than Nc50 for both the LW and SW radiation in the subtropics at 20° latitude. This is a larger positive SW radiative feedback and a larger negative LW radiative feedback. This situation is analogous to the tropical feedbacks seen in Fig. 6.

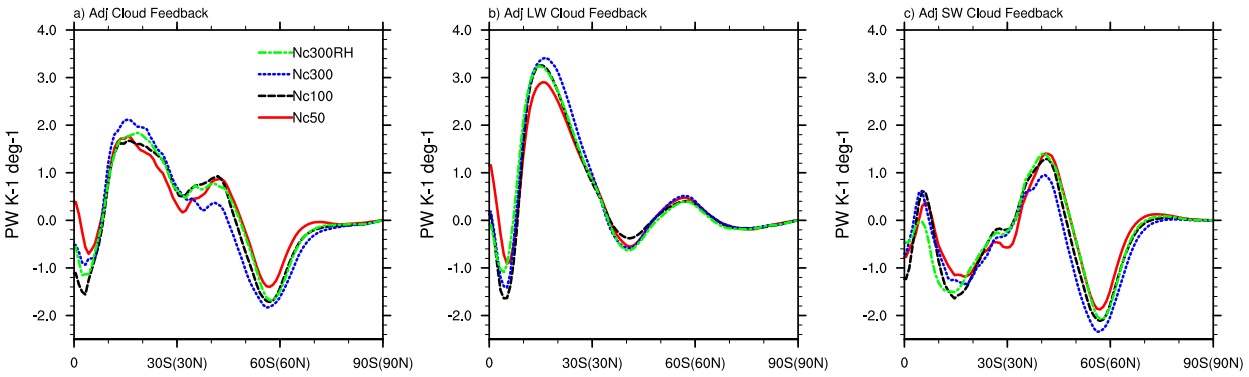

FIG. 9. Zonal-mean (a) total (LW + SW), (b) LW, and (c) SW kernel-adjusted cloud feedback [PW K^{-1} (° lat)$^{-1}$] from aquaplanet simulations. Northern and Southern Hemispheres are averaged (since they are symmetric). Feedbacks are estimated as the difference between a control case and an SST + 4 K case with doubled CO_2. Shown are simulations with fixed N_c of 50 (red solid), 100 (black dashed), and 300 (blue dotted) cm^{-3}, including 300 cm^{-3} but tuned to match the $N_c = 50$ case (green).

Thus the aquaplanet experiments do imply different tropical (or subtropical) cloud feedbacks with drop number: higher positive LW and less negative SW radiative feedbacks as drop number increases (Fig. 9). This occurs because of much larger increases in LWP in the Nc300 and Nc300RH simulation than Nc50. Midlatitude LWP increases 25% more than Nc50. Cloud coverage changes have a very similar structure, and are very similar between Nc50 and Nc300, but slightly larger (because of lower base cloud cover) in Nc300RH. In the global integral, net cloud feedbacks in aquaplanet simulations with higher LWP have larger negative SW cloud radiative feedbacks, and similar LW cloud feedbacks (Table 2). This is mostly an extratropical effect in these simulations, resulting in a difference of 40% in SW cloud radiative feedbacks, or 0.2 W m^{-2} K^{-1}. Because of different regime extents in the aquaplanet these values do not quantitatively translate directly to the Earth-like configuration.

We have analyzed the aquaplanet feedbacks sorted by ω_{500} as in Fig. 8 for the full coupled model simulations. The structure of feedbacks is very different as a function of ω_{500}, with negative net feedback throughout the upwelling regime ($\omega_{500} < 0$). This is similar to the aquaplanet results of Medeiros et al. (2015, their Fig. 8). There is not a clear separation in feedbacks by vertical velocity in the aquaplanet simulations between simulations with high and low drop numbers, except in moderate subsidence regimes ($20 < \omega_{500} < 40$ hPa day^{-1}). Thus the aquaplanet results are different enough in dynamical regime that the effects of different drop number when sorted by regime are hard to ascertain.

5. Results: Aerosol feedback

In the Southern Ocean, the LE simulation has reduced positive cloud feedbacks (Fig. 6) compared to the ME and FixA simulations. This might be related to aerosol changes in the Southern Ocean in Fig. 2, and are not directly forced by emissions changes, so they constitute an aerosol feedback. To quantify the aerosol feedback, aerosol changes due to climate that affect the radiative forcing, we focus on the region of difference in AOD between about 60° and 15°S. Estimating the difference between the ME or FixA simulation feedbacks and the LE simulation in this region (including some negative and positive feedbacks) yields a difference in global cloud feedbacks of -0.06 W m^{-2} K^{-1} between LE and FixA simulations (Table 1), or about 15% of the global cloud feedback in the LE.

Figure 10 illustrates the LWP changes for the different ensembles. LWP change is often correlated with aerosol effects in CESM (Gettelman 2015). In climate change simulations, LWP change contributes to cloud feedbacks with midlatitude warming (Kay et al. 2014a). LWP changes are driven by changes in aerosols and by changes in climate. Warmer climates have higher LWP, and increases in aerosols also increase LWP. Note the correspondence between Figs. 2b and 10b. The Northern Hemisphere changes are largely a result of variable anthropogenic aerosol emissions, with a small component in the subtropics from dust emissions. Dust increases in all simulations within 2060–80 by about 10% at 30°N (not shown) and slightly more in the LE and ME simulations than the FixA ensemble. But note also that LWP increases in the warmer (future) simulations in the Southern Hemisphere, where there is basically no change in anthropogenic emissions. The LE simulation with more warming has significantly larger changes in AOD (Fig. 2) and LWP (Fig. 10) than either the FixA or ME simulation. This results in weaker cloud feedbacks, particularly at their 40°S peak.

TABLE 2. Statistics for aquaplanet simulations illustrating the base state net cloud radiative effect (NetCRE; LW + SW), base state total cloud fraction (CldTot), base state LWP, change in LWP (ΔLWP), and kernel-adjusted cloud feedback for LW, SW, and net radiation.

Simulation	NetCRE ($W m^{-2}$)	CldTot (%)	LWP ($g m^{-2}$)	ΔLWP (%)	Cloud feedback ($W m^{-2} K^{-1}$)		
					LW	SW	Net
Nc50	−34.1	67.5	48.4	+40%	0.47	−0.27	0.20
Nc100	−37.8	67.0	57.5	+46%	0.45	−0.37	0.08
Nc300	−43.7	66.4	71.8	+53%	0.52	−0.48	0.04
Nc300RH	−35.5	64.7	62.0	+54%	0.47	−0.33	0.14

Aquaplanet simulations are also consistent with this aerosol feedback and increase in LWP. There is evidence of larger negative feedbacks in the larger drop number run poleward of the peak in the storm track in Fig. 9. These are also similar to larger feedbacks due to the SW radiation seen in Fig. 6, and also noted by Gettelman et al. (2013). These feedbacks are affected by cloud microphysics and the transition to more liquid in a warmer world. Smaller and more numerous cloud drops are brighter, with a larger SW radiative feedback, and the correspondence of the Nc300 and Nc300RH aquaplanet simulations indicates it is independent of LWP. This feature is seen only in the Southern Hemisphere in a full simulation (Fig. 6) as it is mostly ocean and similar to the aquaplanet.

These changes likely reflect an aerosol feedback, whereby the change in climate affects the aerosol population, which in turn affects the response of clouds. A detailed analysis of the difference between the LE and FixA simulated climates indicates that the LE simulation has higher near-surface wind speed in the Southern Ocean, which would tend to increase sea salt emissions and AOD, leading to larger LWP and increased cloud drop number concentration, damping any reductions in cloud due to warming, and implying a negative aerosol feedback in the Southern Ocean. As noted above, the aerosol feedback is estimated at about 15% of the total cloud feedback in CESM1.

6. Discussion and conclusions

a. *Feedbacks across ensembles*

Feedbacks are nearly identical between the ME (RCP4.5) and LE (RCP8.5) simulations. The similarity confirms that feedback strengths are nearly invariant for a range of plausible future climate forcing. Albedo feedbacks are slightly higher regionally in the

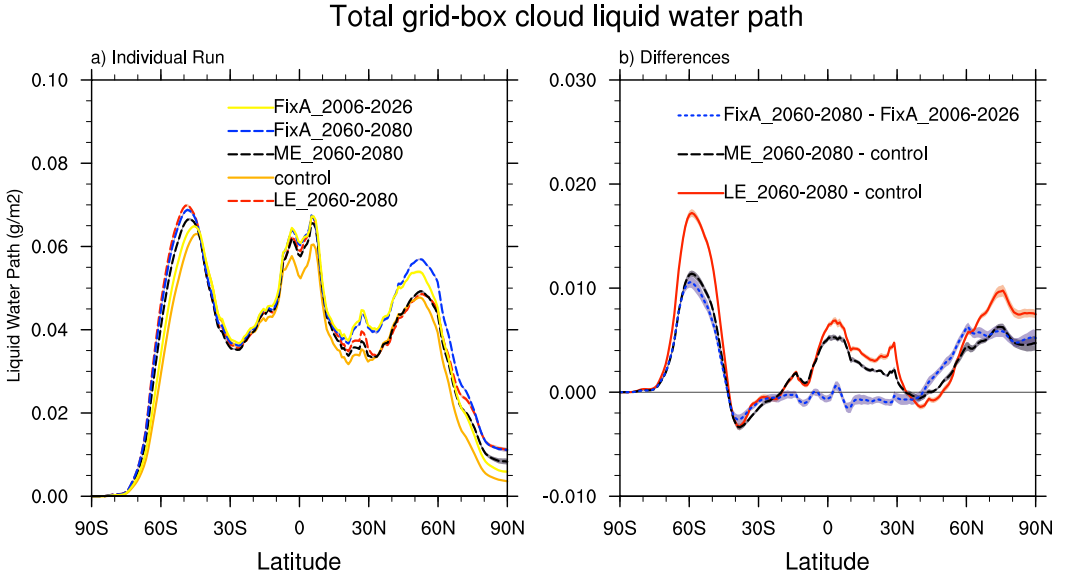

FIG. 10. (a) Zonal-mean liquid water path and (b) zonal-mean liquid water path change from three ensemble simulations: LE (red), ME (black), and FixA (blue). Additional base cases are shown in (a) for the LE and ME control (orange) and the FixA baseline from 2006 to 2026 (yellow). Two standard deviations of zonal-mean adjusted cloud feedback across the ensembles are shown by the shaded regions in (b).

LE (RCP8.5) simulation. This makes sense as high latitudes experience the largest warming.

The ensemble spread (internal variability) in feedbacks is very small. This might be expected for water vapor feedbacks, and possibly even for cloud feedbacks, but it is also true of albedo feedbacks. All feedbacks are remarkably stable with respect to internal variability in a model, even for simulations based on 20 years of output. Low variability of albedo feedbacks may seem counterintuitive in light of work showing large differences in short-term climate trends (Deser et al. 2012; Kay et al. 2014b). Variability in near-term climate trends is not caused by varying feedbacks. It implies that the variability in high-latitude warming trends is due more to variations in heat transport or absorption or constant feedback responses of the coupled system (heat to or from the ocean) than to variations in the structural nature of ''fast feedbacks'' in the atmosphere or at the surface. Even large-scale decadal modes of variability do not seem to project onto feedbacks.

b. *Role of aerosols in feedbacks*

The role of aerosols in climate feedbacks is complex. Aerosols alias into cloud feedbacks, and in simulations with changing aerosols they must be accounted for. As an added complication, the efficiency (or efficacy) of inhomogeneous forcing like aerosols to affect surface temperature may be larger than that for CO_2 (Hansen et al. 2005; Shindell 2014; Marvel et al. 2015). Different efficacies may bias the estimates of total response from historical forcing. Here we have shown a complementary result: aerosol forcings alter interpretations of future climate feedbacks, not just present-day forcing. We use an equilibrium framework, similar to effective radiative forcing (Marvel et al. 2015), where efficacies for aerosols are close to 1.

The aerosol kernel method is largely successful at removing a signal due to aerosols in the different ensembles, and the resulting cloud feedbacks including an aerosol kernel adjustment are quite similar in many regions. However, it is difficult to apply a single aerosol kernel across models. The aerosol kernel is basically an expression of the ACI in a particular model. A comparison of aerosol kernels across models would be a useful framework for analyzing multimodel uncertainty in ACI.

In addition to the spurious changes that aerosols will have because of ACI from changes in emissions, there are other changes we have not removed. These changes in feedbacks remain because they are not present in the aerosol emissions change experiment from which the kernel was calculated. There are two effects due to cloud state changes and aerosol feedbacks.

c. *Cloud state changes from aerosols*

First, aerosols affect cloud feedbacks through effects of altering the cloud state. The difference is evident in the tropics of the CESM simulations, where cloud feedbacks, adjusted for aerosols, are still higher in tropics and subtropics in the FixA ensemble than in the LE and ME simulations. The difference is 0.07–0.08 $W m^{-2} K^{-1}$, or approximately 20% of the total global cloud feedback. For a typical total feedback parameter of 1.33 $W m^{-2} K^{-1}$, implying a 3-K climate sensitivity for a 4 $W m^{-2}$ CO_2 forcing, the difference would contribute to about 0.25 K of climate sensitivity. This is much larger than the variance in the feedbacks within any ensemble, so the difference is not internal variability of simulations. In general the LW radiative feedbacks are more positive, and the SW radiation less negative with higher aerosols. In the tropics the increase in feedback occurs in most regions. In midlatitudes, there are offsetting changes between land and ocean: ocean regions see more positive feedback in the NH in the FixA ensemble, but the zonal-mean total cloud feedback is similar.

How certain are these effects, and what is the mechanism? The higher feedbacks are seen with and without the aerosol kernel adjustment. The effects are substantial in regions of eastern and southeastern Asia, as well as over the subtropical oceans (Fig. 7), where higher aerosols in the FixA ensemble brighten clouds throughout the twenty-first century. The effect may be through reduced LWP change and different base state LWP, which may buffer changes in SW radiative cloud cover and increase SW radiative feedbacks, or increase high clouds in the tropics and affect the ice phase. A more detailed analysis with cloud property kernels and using other models with different aerosol treatments would be valuable for understanding the mechanisms further.

Altered feedbacks due to different cloud state are seen in aquaplanet simulations. The different drop number experiments are an analog for higher aerosol concentrations. The regimes are different than in the full simulations, but the subtropical increase in feedbacks occurs with higher drop numbers, with LW radiation increases not quite balanced by SW radiation decreases because of larger changes in high clouds in the higher drop number experiments. In full simulations, the main signal in the tropics is a high cloud effect over land, the Maritime Continent and some ocean regions. Aquaplanet simulations have higher LWP with larger drop numbers (unless LWP limited as in Nc300RH) and larger cloud feedbacks as LWP increases. Different drop numbers alter LWP in the aquaplanet simulations,

and the change in LWP seems to alter cloud feedbacks. Note that LWP is adjusted with the Nc300RH simulation to be more like Nc50, and the resulting feedbacks are more like Nc50. The mechanism is consistent with full simulations where aerosols alter LWP.

d. Aerosol feedback

The second effect of aerosols is an ''aerosol feedback'' that results from aerosols whose emissions depend on climate. In the Southern Hemisphere storm tracks there appears to be a feedback based on increasing wind speed increasing sea salt, and this increases drop number and cloud brightness, hence creating a different feedback. This contributes about 15% of total cloud feedback (0.04–0.06 $W m^{-2} K^{-1}$), and this difference would imply about 0.15 K of global mean surface temperature change. No significant effect is seen with dust emissions, which affect a region of the subtropics, but have a smaller perturbation.

e. Conclusions

In summary, climate feedbacks are remarkably stable across ensemble members, even when estimated using only 20 years of data (as with the FixA simulation). Variance reaches only 25% of the feedback in highly variable regions such as the sea ice edge for albedo feedbacks, and the subtropics for water vapor feedbacks. Cloud feedbacks have regional variance up to 30% of the local cloud feedback, but the global variance is very small (5%).

It is possible to calculate feedbacks with transient simulations, and feedbacks estimated with different RCPs (LE vs ME simulations) are nearly identical in all respects. Thus feedbacks are broadly linear for perturbations on the century time scale.

Changing aerosol emissions will change cloud radiative effects and alias into climate feedbacks. These must be removed to understand what the true cloud feedback is, which can be accomplished with an ''aerosol kernel.'' There appears to be a small impact of different cloud microphysical states (induced by aerosols, and specified in the aquaplanet simulations) on cloud feedbacks, mostly through the longwave effect of high clouds in the tropics, which in CESM is approximately 20% of the global cloud feedback.

There also appear to be distinct aerosol feedbacks from aerosol species whose emissions are dependent on climate. Here the warmer climate of the RCP8.5 LE simulation has higher wind speeds than in the control climate, and thus larger AOD from sea salt, leading to a change in drop number and an impact on clouds. The Southern Ocean aerosol feedback in CESM is about 15% of the global cloud feedback. In the midlatitudes of the aquaplanet simulations, cloud feedbacks are similarly altered by specifying higher drop numbers.

Aquaplanet simulations show sensitivity to drop number, with extratropical SW cloud feedbacks getting more negative with higher LWP. The regimes are different than in full simulations, making direct attribution difficult. However, the simulations confirm that cloud microphysics and aerosol effects on cloud microphysics may alter cloud feedbacks.

Thus aerosol effects need to be accounted for in complex Earth system models (ESMs), and comparisons across models will have uncertainties in cloud feedback driven by differences in aerosols and aerosol–cloud interactions. In CESM, the combined effects of aerosol feedback and alterations to cloud feedback contribute to a nearly 50% difference in total cloud feedback between the LE (0.41 $W m^{-2} K^{-1}$) and FixA (0.60 $W m^{-2} K^{-1}$) simulations (Table 1), regardless of aerosol kernel used. Aerosols may enhance ensemble spread across multimodel ensembles due to different treatments of aerosols and aerosol–cloud interactions. These mechanisms and effects should be verified in other ESMs with comprehensive aerosol treatments, and further detailed and idealized experiments conducted to more completely isolate and quantify aerosol feedbacks.

Acknowledgments. Thanks to B. Sanderson and J. Fasullo for comments. L. Lin is supported by the National Basic Research Program of China (2012CB955303), NSFC Grant 41275070, the National Science Foundation of China under Grant (41405010), and the China Scholarship council. B. Medeiros and J. Olson acknowledge support from the Regional and Global Climate Modeling Program of the U.S. Department of Energy's Office of Science, Cooperative Agreement DE-FC02-97ER62402.

REFERENCES

Albrecht, B. A., 1989: Aerosols, cloud microphysics and fractional cloudiness. *Science*, **245**, 1227–1230, doi:10.1126/science.245.4923.1227.

Armour, K. C., C. M. Bitz, and G. H. Roe, 2013: Time-varying climate sensitivity from regional feedbacks. *J. Climate*, **26**, 4518–4534, doi:10.1175/JCLI-D-12-00544.1.

Bony, S., and J. L. Dufresne, 2005: Marine boundary layer clouds at the heart of tropical cloud feedback uncertainties in climate models. *Geophys. Res. Lett.*, **32**, L20806, doi:10.1029/2005GL023851.

——, and Coauthors, 2015: Clouds, circulation and climate sensitivity. *Nat. Geosci.*, **8**, 261–268, doi:10.1038/ngeo2398.

Boucher, O., and Coauthors, 2013: Clouds and aerosols. *Climate Change 2013: The Physical Science Basis*, T. F. Stocker et al., Eds., Cambridge University Press, 571–657.

Cess, R. D., and Coauthors, 1990: Intercomparison and interpretation of climate feedback processes in 19 atmospheric general circulation models. *J. Geophys. Res.*, **95**, 16 601–16 615, doi:10.1029/JD095iD10p16601.

Deser, C., A. Phillips, V. Bourdette, and H. Teng, 2012: Uncertainty in climate change projections: The role of internal variability. *Climate Dyn.*, **38**, 527–546, doi:10.1007/s00382-010-0977-x.

Dessler, A. E., 2010: A determination of the cloud feedback from climate variations over the past decade. *Science*, **330**, 1523–1527, doi:10.1126/science.1192546.

Fasullo, J. T., B. M. Sanderson, and K. E. Trenberth, 2015: Recent progress in constraining climate sensitivity with model ensembles. *Curr. Climate Change Rep.*, **1**, 268–275, doi:10.1007/s40641-015-0021-7.

Flato, G., and Coauthors, 2013: Evaluation of climate models. *Climate Change 2013: The Physical Science Basis*, T. F. Stocker et al., Eds., Cambridge University Press, 741–866.

Forster, P. M. F., and J. M. Gregory, 2006: The climate sensitivity and its components diagnosed from Earth radiation budget data. *J. Climate*, **19**, 39–52, doi:10.1175/JCLI3611.1.

Gettelman, A., 2015: Putting the clouds back in aerosol–cloud interactions. *Atmos. Chem. Phys.*, **15**, 12 397–12 411, doi:10.5194/acp-15-12397-2015.

——, and H. Morrison, 2015: Advanced two-moment bulk microphysics for global models. Part I: Off-line tests and comparison with other schemes. *J. Climate*, **28**, 1268–1287, doi:10.1175/JCLI-D-14-00102.1.

——, and Coauthors, 2010: Global simulations of ice nucleation and ice supersaturation with an improved cloud scheme in the Community Atmosphere Model. *J. Geophys. Res.*, **115**, D18216, doi:10.1029/2009JD013797.

——, J. E. Kay, and K. M. Shell, 2012a: The evolution of climate feedbacks in the Community Atmosphere Model. *J. Climate*, **25**, 1453–1469, doi:10.1175/JCLI-D-11-00197.1.

——, X. Liu, D. Barahona, U. Lohmann, and C. C. Chen, 2012b: Climate impacts of ice nucleation. *J. Geophys. Res.*, **117**, D20201, doi:10.1029/2012JD017950.

——, H. Morrison, C. R. Terai, and R. Wood, 2013: Microphysical process rates and global aerosol–cloud interactions. *Atmos. Chem. Phys.*, **13**, 9855–9867, doi:10.5194/acp-13-9855-2013.

Ghan, S. J., and Coauthors, 2013: A simple model of global aerosol indirect effects. *J. Geophys. Res. Atmos.*, **118**, 6688–6707, doi:10.1002/jgrd.50567.

Gregory, J. M., and Coauthors, 2004: A new method for diagnosing radiative forcing and climate sensitivity. *Geophys. Res. Lett.*, **31**, L03205, doi:10.1029/2003GL018747.

Hansen, J., and Coauthors, 2005: Efficacy of climate forcings. *J. Geophys. Res.*, **110**, D18104, doi:10.1029/2005JD005776.

Jonko, A. K., K. M. Shell, B. M. Sanderson, and G. Danabasoglu, 2012: Climate feedbacks in CCSM3 under changing CO_2 forcing. Part I: Adapting the linear radiative kernel technique to feedback calculations for a broad range of forcings. *J. Climate*, **25**, 5260–5272, doi:10.1175/JCLI-D-11-00524.1.

Kay, J. E., B. Medeiros, Y.-T. Hwang, A. Gettelman, J. Perket, and M. Flanner, 2014a: Processes controlling Southern Ocean shortwave climate feedbacks in CESM. *Geophys. Res. Lett.*, **41**, 616–622, doi:10.1002/2013GL058315.

——, and Coauthors, 2014b: The Community Earth System Model (CESM) Large Ensemble Project: A community resource for studying climate change in the presence of internal climate variability. *Bull. Amer. Meteor. Soc.*, **96**, 1333–1349, doi:10.1175/BAMS-D-13-00255.1.

Klocke, D., J. Quaas, and B. Stevens, 2013: Assessment of different metrics for physical climate feedbacks. *Climate Dyn.*, **41**, 1173–1185, doi:10.1007/s00382-013-1757-1.

Knutti, R., and M. A. A. Rugenstein, 2015: Feedbacks, climate sensitivity and the limits of linear models. *Philos. Trans. Roy. Soc.*, **373A**, doi:10.1098/rsta.2015.0146.

Lamarque, J., G. Kyle, M. Meinshausen, K. Riahi, S. Smith, D. van Vuuren, A. Conley, and F. Vitt, 2011: Global and regional evolution of short-lived radiatively-active gases and aerosols in the representative concentration pathways. *Climatic Change*, **109**, 191–212, doi:10.1007/s10584-011-0155-0.

Liu, X., and Coauthors, 2012: Toward a minimal representation of aerosols in climate models: Description and evaluation in the Community Atmosphere Model CAM5. *Geosci. Model Dev.*, **5**, 709–739, doi:10.5194/gmd-5-709-2012.

Marvel, K., G. A. Schmidt, R. L. Miller, and L. S. Nazarenko, 2015: Implications for climate sensitivity from the response to individual forcings. *Nat. Climate Change*, **6**, 386–389, doi:10.1038/nclimate2888.

Medeiros, B., B. Stevens, and S. Bony, 2015: Using aquaplanets to understand the robust responses of comprehensive climate models to forcing. *Climate Dyn.*, **44**, 1957–1977, doi:10.1007/s00382-014-2138-0.

——, D. L. Williamson, and J. G. Olson, 2016: Reference aquaplanet climate in the Community Atmosphere Model, version 5. *J. Adv. Model. Earth Syst.*, **8**, 406–424, doi:10.1002/2015MS000593.

Neale, R. B., and Coauthors, 2010: Description of the NCAR Community Atmosphere Model (CAM5.0). NCAR Tech. Rep. NCAR/TN-486+STR, 268 pp.

Park, S., 2014: A Unified Convection Scheme (UNICON). Part I: Formulation. *J. Atmos. Sci.*, **71**, 3902–3930, doi:10.1175/JAS-D-13-0233.1.

Sanderson, B. M., K. W. Oleson, W. G. Strand, F. Lehner, and B. C. O'Neill, 2016: A new ensemble of GCM simulations to assess avoided impacts in a climate mitigation scenario. *Climatic Change*, doi:10.1007/s10584-015-1567-z, in press.

Schneider, S., 1972: Cloudiness as a global climatic feedback mechanism: The effects on radiation balance and surface temperatures of variations in cloudiness. *J. Atmos. Sci.*, **29**, 1413–1422, doi:10.1175/1520-0469(1972)029<1413:CAAGCF>2.0.CO;2.

Shell, K. M., J. T. Kiehl, and C. A. Shields, 2008: Using the radiative kernel technique to calculate climate feedbacks in NCAR's Community Atmosphere Model. *J. Climate*, **21**, 2269–2282, doi:10.1175/2007JCLI2044.1.

Shindell, D. T., 2014: Inhomogeneous forcing and transient climate sensitivity. *Nat. Climate Change*, **4**, 274–277, doi:10.1038/nclimate2136.

Soden, B. J., I. M. Held, R. Colman, K. M. Shell, J. T. Kiehl, and C. A. Shields, 2008: Quantifying climate feedbacks using radiative kernels. *J. Climate*, **21**, 3504–3520, doi:10.1175/2007JCLI2110.1.

Twomey, S., 1977: The influence of pollution on the shortwave albedo of clouds. *J. Atmos. Sci.*, **34**, 1149–1152, doi:10.1175/1520-0469(1977)034<1149:TIOPOT>2.0.CO;2.

van Vuuren, D. P., and Coauthors, 2011: The representative concentration pathways: An overview. *Climatic Change*, **109**, 5–31, doi:10.1007/s10584-011-0148-z.

Xu, Y., J.-F. Lamarque, and B. M. Sanderson, 2016: The importance of aerosol scenarios in projections of future heat extremes. *Climatic Change*, doi:10.1007/s10584-015-1565-1, in press.

Zelinka, M., S. Klein, and D. Hartmann, 2012: Computing and partitioning cloud feedbacks using cloud property histograms. Part II: Attribution to changes in cloud amount, altitude, and optical depth. *J. Climate*, **25**, 3736–3754, doi:10.1175/JCLI-D-11-00249.1.